BMC Genomics

RESEARCH

Open Access

Integrated miRNA-seq and functional analyses reveal the regulatory role of sha-miR-92a_L+2R+4 via targeting *vegfaa* in rainbow trout (*Oncorhynchus mykiss*) responding to acute hypoxia and reoxygenation stress

Yongjuan Li[1,2], Shenji Wu[1], Jinqiang Huang[1*] and Lu Zhao[1]

Abstract

Background Hypoxia negatively affects the behavior, growth, reproduction and survival of fish, causing serious economic losses to aquaculture. Rainbow trout (*Oncorhynchus mykiss*), an important economic fish worldwide, belongs to a hypoxia-sensitive fish species, however, little is known about the regulatory mechanism of microRNAs (miRNAs) under hypoxia stress.

Results Rainbow trout were subjected to hypoxia stress for 3 h (H3h_L), 12 h (H12h_L), 24 h (H24h_L) and 3 h reoxygenation (R3h_L) to systemically evaluate the changes of miRNA expression profiles in liver, and functions of sha-miR-92a_L+2R+4 were investigated. We found 17, 144, 57 and 55 differentially expressed (DE) miRNAs in the H3h_L vs. control (N_L), H12h_L vs. N_L, H24h_L vs. N_L and R3h_L vs. N_L comparisons, respectively. Enrichment analysis revealed that the targets of DE miRNAs were significantly enriched in HIF signaling pathway, VEGF signaling pathway, FoxO signaling pathway and glycolysis/gluconeogenesis. Through miRNA-mRNA interaction and weighted gene co-expression network analysis (WGCNA), five key DE miRNAs (sha-miR-92a_L+2R+4, ssa-miR-128-3p, ssa-miR-101b-3p_R+1, ola-miR-199a-5p_R+2 and tni-miR-199_1ss18CG) were identified, which can target at least two hypoxia-responsive genes, such as *vegfaa*, *ho*, *glut1a* and *junb*. Functional analysis found that sha-miR-92a_L+2R+4 directly regulated *vegfaa* expression by targeting its 3′-UTR, overexpression of sha-miR-92a_L+2R+4 significantly decreased *vegfaa* expression in rainbow trout liver cells, while opposite results were obtained after transfection of sha-miR-92a_L+2R+4 inhibitor. Furthermore, overexpressed sha-miR-92a_L+2R+4 promoted rainbow trout liver cell proliferation and inhibited apoptosis.

Conclusion This study deepens our understanding of the crucial roles of miRNAs under hypoxia stress in rainbow trout. These results can contribute to devise strategies for improving rainbow trout survival rate and aquaculture production during hypoxia stress and help speeding up the selective breeding of hypoxia-tolerant rainbow trout.

*Correspondence:
Jinqiang Huang
huangjinq@163.com
[1]College of Animal Science and Technology, Gansu Agricultural University, Lanzhou 730070, China
[2]College of Science, Gansu Agricultural University, Lanzhou 730070, China

Keywords Rainbow trout, Hypoxia, sha-miR-92a_L+2R+4, *vegfaa*

Introduction

Dissolved oxygen (DO) is a key limiting ecological factor affecting fisheries production because energy metabolism, normal growth and reproduction of fish require DO at efficient levels [1, 2]. DO level in water is unstable and susceptible to water quality, weather variations, temperature and cultivation density, resulting in frequent exposure of fish to hypoxic environments [3]. This unfavorable aquatic habitat can induce fish hypoxia response, which has maximum adverse effects on behavior, physiology, growth and survival [4]. What's worse, fish reduce their resistance versus other environmental stress under hypoxic conditions, such as high temperature, salinity and pathogen infection [5–7]. With water pollution and global warming more serious, hypoxia has become increasingly problematic since hypoxia are gradually rising every year in the aquaculture industry. Consequently, it is urgent to uncover the molecular mechanisms of fish hypoxia adaptation.

In view of the importance to actual aquaculture production, the molecular mechanisms of fish responding to hypoxia have garnered substantial attention in recent years, and key hypoxia-related pathways have been gradually reported, showing that hypoxia-inducible factor 1 (HIF-1), forkhead box O (FoxO), mitogen-activated protein kinase (MAPK), AMP-activated protein kinase (AMPK) and tumor suppressor protein P53 (P53) signaling pathways performed pivotal roles in response to hypoxia stress [8–10]. The especially interesting fact is that microRNAs (miRNAs), a group of small noncoding RNAs between 19 and 25 nucleotides (nt) that can regulate gene expression at the post-transcriptional level, are involved in hypoxia response of fish [11, 12]. Through comparative transcriptome data analysis, a number of miRNAs from catfish (*Pelteobagrus vachelli*) [13], silver carp (*Hypophthalmichthys molitrix*) [14], cobia (*Rachycentron canadum*) [15] and crucian carp (*Carassius auratus*) [16], were widely modulated under hypoxia stress. These modulated miRNAs induced by hypoxia exhibited their functions on controlling energy metabolism, immune response and apoptosis, and the regulation of these functions strengthened hypoxia tolerance. Furthermore, dozens of target genes regulated by hypoxia-related miRNAs have been identified. For examples, a study in Nile tilapia (*Oreochromis niloticus*) has reported that miR-204 loss of function could influence blood O_2-carrying capacity, anaerobic metabolism and antioxidant enzyme activity via targeting vascular endothelial growth factor (*vegf*) [17]. In zebrafish (*Danio rerio*), Huang et al. [18] found that overexpression of miR-462 and miR-731 blocked cell cycle progress under hypoxia by negative regulation of DEAD (Asp-Glu-Ala-Asp) box helicase 5 (*ddx5*) and protein phosphatase, Mg^{2+}/Mn^{2+} dependent, 1 Da (*ppm1da*) expression, respectively. Also, in tilapia under hypoxia stress, miR-34a was shown to participate in the regulation of HIF-1 and P53 signaling pathways activity via targeting glucose transporter 1 (*glut1*) [10]. Apparently, miRNAs regulation of hypoxia-responsive genes is a key mechanism of fish in response to hypoxia, and the study of hypoxia-related miRNAs is essential to excavate the molecular mechanisms of hypoxia adaptation in fish.

Despite the evidence for the hypoxia-related regulatory functions of miRNAs, few studies have been executed on rainbow trout (*Oncorhynchus mykiss*) [19–21]. Rainbow trout, which is an important cold water fish with great economic value, has been widely cultured around the world. Compared with most fish, rainbow trout (lethal hypoxia, 3.0 mg/L) is more sensitive to hypoxia, making it a unique model species for studying hypoxia stress [1]. Nowadays, in addition to the severe effects of global warming, the shift in rainbow trout culture mode from large-scale farming to high density pond refinement caused by increased consumer demand inevitably exposes rainbow trout to hypoxic environments regularly, which severely limits rainbow trout aquaculture. Previous report showed that hypoxia could aggravate the toxicity of ammonia nitrogen in rainbow trout besides negative effects on behavior, physiology and growth rate, which greatly affects the health of farmed rainbow trout [22]. The study of the molecular mechanisms of rainbow trout under hypoxia stress will be useful to explore optimal culture conditions.

The liver, which is the most critical metabolic organ of the body, is extremely sensitive to hypoxia, and a large number of gene transcription events involved in angiogenesis, erythropoiesis, glucose absorption and metabolism occur when liver cells and tissues are in a state of hypoxia [23]. Interestingly, reoxygenation after hypoxia has also been shown to cause hepatic oxidative damage and apoptosis [24, 25]. In the present study, the miRNA expression profile changes in the liver of rainbow trout under hypoxia for different durations and reoxygenation stress were detected using the Illumina HiSeq 2500 sequencing platform, and the functions of sha-miR-92a_L+2R+4 were further investigated. The results of this study expand our knowledge about the regulatory roles of miRNAs under hypoxia stress in rainbow trout, and provide useful resources for breeding hypoxia-tolerant rainbow trout.

Results

Sequencing overview of miRNA

The miRNA-seq from the 15 libraries generated 179,674,302 raw reads with an average of 11,978,287 reads per sample, and the data has been deposited in the National Center for Biotechnology Information (NCBI) database (GSE231752). After filtering the raw reads, 33,269,429, 30,255,183, 36,692,418, 28,725,825 and 28,871,165 clean reads were obtained from N_L, H3h_L, H12h_L, H24h_L and R3h_L, respectively, accounting for 86.82%, 86.85%, 92.72%, 85.85% and 86.21% of total reads (Table 1). The length distributions of miRNAs showed that a majority of the miRNAs were 21–23 nt, of which 22 nt miRNAs accounted for the largest proportion, representing 31.29% (N_L), 27.07% (H3h_L), 38.94% (H12h_L), 35.93% (H24h_L) and 35.96% (R3h_L), respectively (Fig. 1A). Besides, the miRNA expression in the biological triplicates displayed Pearson's correlation coefficients > 0.88, revealing a high repeatability between the samples in the five groups (Fig. S1).

Identification of DE miRNAs

A total of 1356, 1349, 1407, 1510 miRNAs were obtained from the H3h_L vs. N_L, H12h_L vs. N_L, H24h_L vs. N_L and R3h_L vs. N_L comparisons, respectively, and their overall expression levels in each group were compared (Fig. 1B). Based on $|\text{Log}_2$ fold change $| > 1$ and p-value < 0.05 as thresholds, 17 (14 known and 3 novel miRNAs), 144 (123 known and 21 novel miRNAs), 57 (49 known and 8 novel miRNAs) and 55 (42 known and 13 novel miRNAs) miRNAs were identified as DE miRNAs (Table S2). Of these DE miRNAs, 6, 72, 9 and 16 DE miRNAs were upregulated and 11, 72, 48 and 39 were downregulated, respectively (Fig. 1C–F). These results suggested that hypoxia stress resulted in a more severe change at 12 h in rainbow trout with the largest number of DE miRNAs. The upset plot of the DE miRNAs showed that most miRNAs were not expressed in all hypoxia stages (Fig. 1G). In addition, hierarchical clustering analysis was performed on these DE miRNAs in each comparison (Fig. 2A–D).

As determined using short time-series expression miner (STEM), three significant model profiles (Profiles 7, 10 and 11) from the 20 distinct expression patterns were identified. Profiles 7, 10 and 11 contained 45, 28 and 25 DE miRNAs, respectively. The expression level of miRNAs in expression pattern 7 exhibited the lowest value in H12h_L across all five stages, whereas miRNAs in expression patterns 10 and 11 showed significant peaks, which were opposite of the mRNA expression patterns we previously observed (Fig. 2E).

Target prediction of DE miRNAs and integrative analysis

Based on the principle of negative regulation of mRNAs by miRNAs, miRNA-mRNA regulatory networks were constructed using DE miRNAs and DE mRNAs. The results showed that there were 118, 2613, 1016 and 218 negatively correlated miRNA-mRNA pairs in the H3h_L vs. N_L, H12h_L vs. N_L, H24h_L vs. N_L and R3h_L vs. N_L comparisons, respectively, as shown in Table S3. Of these, numerous hypoxia-related target genes were identified, including hypoxia-inducible factor 1α (*hif1α*), vascular endothelial growth factor aa (*vegfaa*), heme oxygenase (*ho*), factor inhibiting hypoxia-inducible factor 1*α* (*fih1*), forkhead box O gene family (*foxo1a*, *foxo3*, *foxo4*), insulin-like growth factor-1 (*igf1*), insulin-like growth factor-binding protein 1 (*igfbp1*), insulin-like growth factor-binding protein 6 (*igfbp6*), dual specificity protein phosphatase 1 (*dusp1*), dual specificity protein phosphatase 8 (*dusp8*), DNA damage-inducible transcript 4 (*ddit4*), transcription factor jun-b (*junb*) and many others involved in glucose metabolism and immunity (Fig. 3).

Table 1 Summary statistics of the miRNA-seq data

Sample name	Raw reads	Clean reads	rRNA	tRNA	SnoRNA	snRNA
N_L1	9,381,969	8,297,529	137,640 (1.47%)	41,968 (0.45%)	6317 (0.07%)	7797 (0.08%)
N_L2	13,697,788	11,861,261	298,882 (2.18%)	132,767 (0.97%)	20,934 (0.15%)	14,048 (0.10%)
N_L3	15,238,767	13,110,639	281,779 (1.85%)	129,409 (0.85%)	18,656 (0.12%)	22,108 (0.15%)
H3h_L1	13,101,909	10,762,587	162,156 (1.24%)	66,071 (0.50%)	12,663 (0.10%)	16,300 (0.12%)
H3h_L2	11,172,963	10,303,556	184,573 (1.65%)	72,314 (0.65%)	10,626 (0.10%)	10,043 (0.09%)
H3h_L3	10,560,382	9,189,040	224,561 (2.13%)	66,358 (0.63%)	13,134 (0.12%)	13,042 (0.12%)
H12h_L1	9,532,057	8,900,500	105,741 (1.11%)	31,497 (0.33%)	2260 (0.02%)	2131 (0.02%)
H12h_L2	15,891,256	14,498,498	176,918 (1.11%)	56,320 (0.35%)	5907 (0.04%)	4133 (0.03%)
H12h_L3	14,148,037	13,293,420	141,913 (1.00%)	40,976 (0.29%)	3748 (0.03%)	4309 (0.03%)
H24h_L1	12,389,853	10,998,696	143,602 (1.16%)	35,012 (0.28%)	5588 (0.05%)	6188 (0.05%)
H24h_L2	12,415,586	10,256,185	180,222 (1.45%)	53,631 (0.43%)	8061 (0.06%)	11,098 (0.09%)
H24h_L3	8,654,001	7,470,944	144,908 (1.67%)	39,279 (0.45%)	7582 (0.09%)	8000 (0.09%)
R3h_L1	14,148,037	12,909,615	137,004 (0.97%)	38,477 (0.27%)	10,361 (0.07%)	9391 (0.07%)
R3h_L2	8,926,370	6,942,135	122,286 (1.37%)	29,980 (0.34%)	6758 (0.08%)	10,084 (0.11%)
R3h_L3	10,415,327	9,019,415	96,813 (0.93%)	24,065 (0.23%)	3644 (0.03%)	5787 (0.06%)

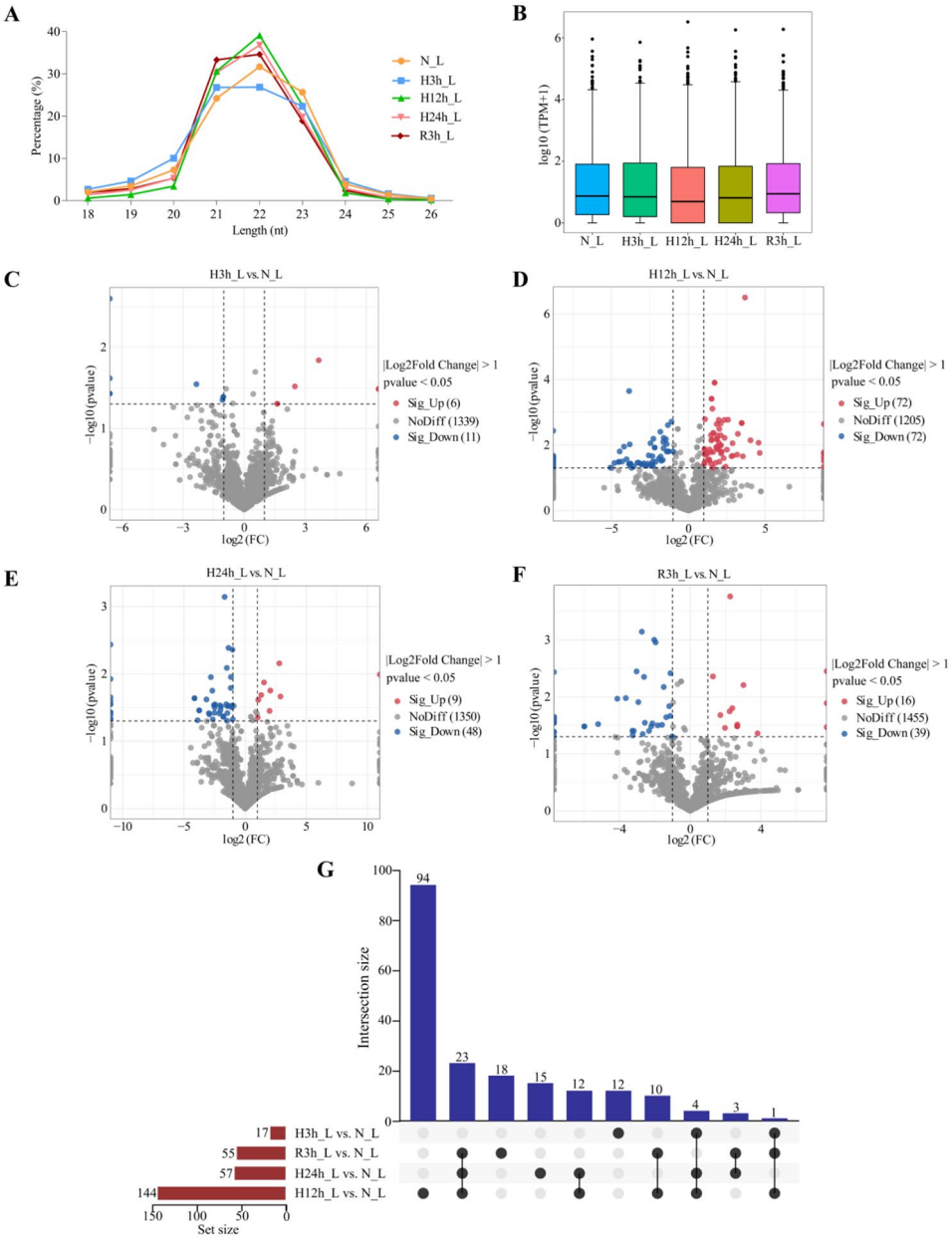

Fig. 1 Sequence and expression characteristics of miRNAs. **(A)** Length distribution of miRNAs in N_L, H3h_L, H12h_L, H24h_L and R3h_L groups. **(B)** Comparison of the overall expression levels of miRNAs among the groups. **(C–F)** Volcano scatter plot of differentially expressed (DE) miRNAs in each comparison group. **(G)** An upset plot of the intersections between pairwise comparisons

In addition, although only one target was identified for most DE miRNAs, some DE miRNAs can target at least two hypoxia-related genes. For example, cfa-miR-323 targeted *foxo3*, *ddit4* and glucokinase (*gck*), and sha-miR-92a_L+2R+4 targeted *vegfaa* and *igfbp6* (Table 2).

GO and KEGG enrichment analysis of target genes

To insight into the different functions of target genes of DE miRNAs under hypoxia stress in rainbow trout, GO assignments were utilized. The results showed that GO analysis consisted of three components: biological process, cellular component and molecular function. Using q-value<0.05 as the threshold, there were 125, 47, 118 and one significantly enriched GO terms in the H3h_L vs. N_L, H12h_L vs. N_L, H24h_L vs. N_L and R3h_L vs. N_L comparisons, respectively (Table S4). In these four comparison groups, the top two biological process items containing the highest number of target genes were 'regulation of transcription, DNA-templated' (GO:0006355) and 'biological_process' (GO:0008150), and 'metabolic process' (GO:0008152) was also enriched by a higher number of target genes; 'nucleus'

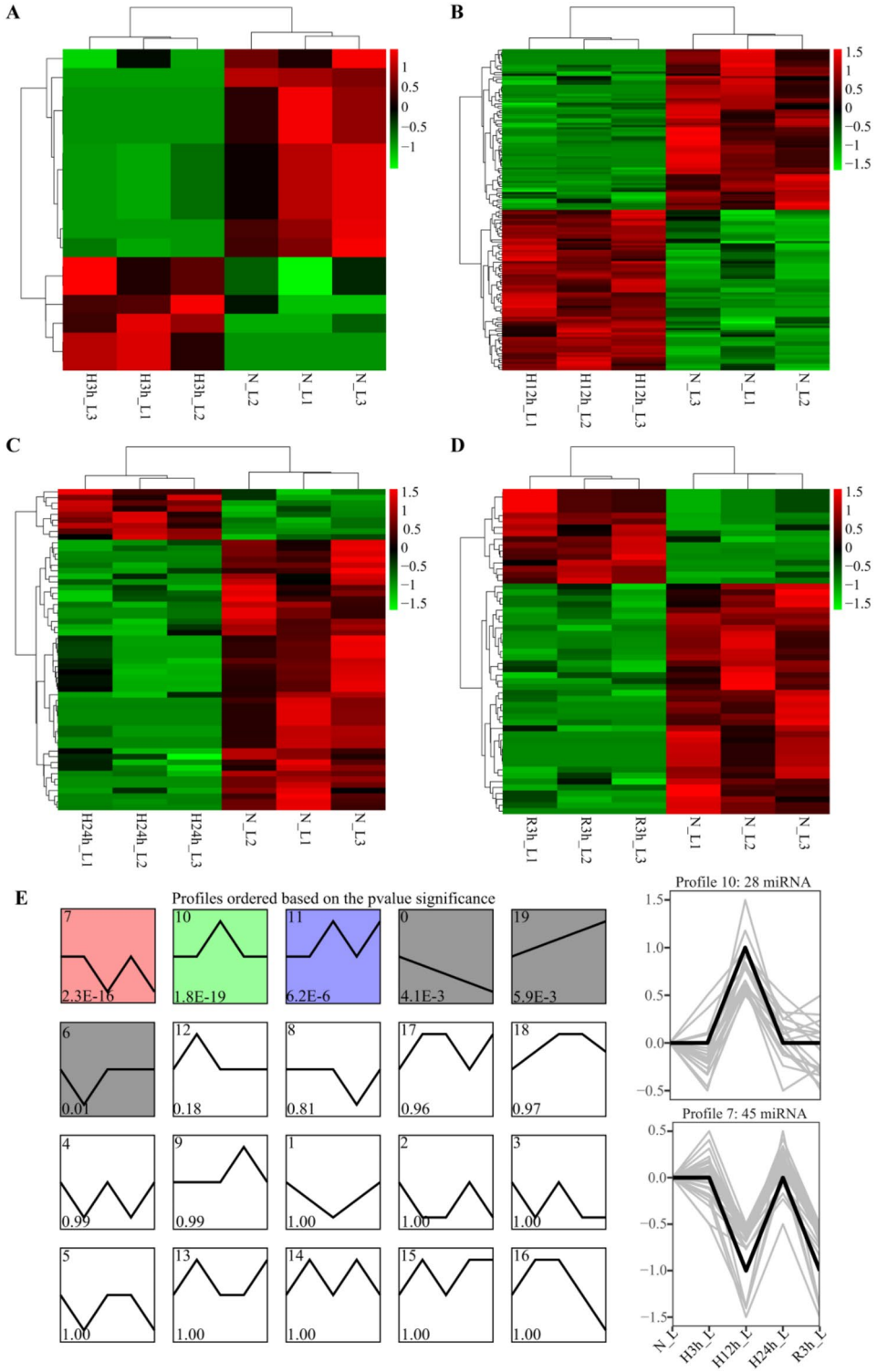

Fig. 2 Hierarchical cluster and STEM analyses of DE miRNAs based on hypoxia exposure time **(A)** H3h_L vs. N_L. **(B)** H12h_L vs. N_L. **(C)** H24h_L vs. N_L. **(D)** R3h_L vs. N_L. **(E)** Short time-series expression profiles

(GO:0005634), 'membrane' (GO:001602) and 'cytoplasm' (GO:0005737) contained the most target genes in cellular component category; 'DNA binding' (GO:0003677) and 'metal ion binding' (GO:0046872) were the most enriched items for target genes in molecular function category (Fig. 4).

In addition, KEGG pathway annotation analysis was performed to better understand the potential functions

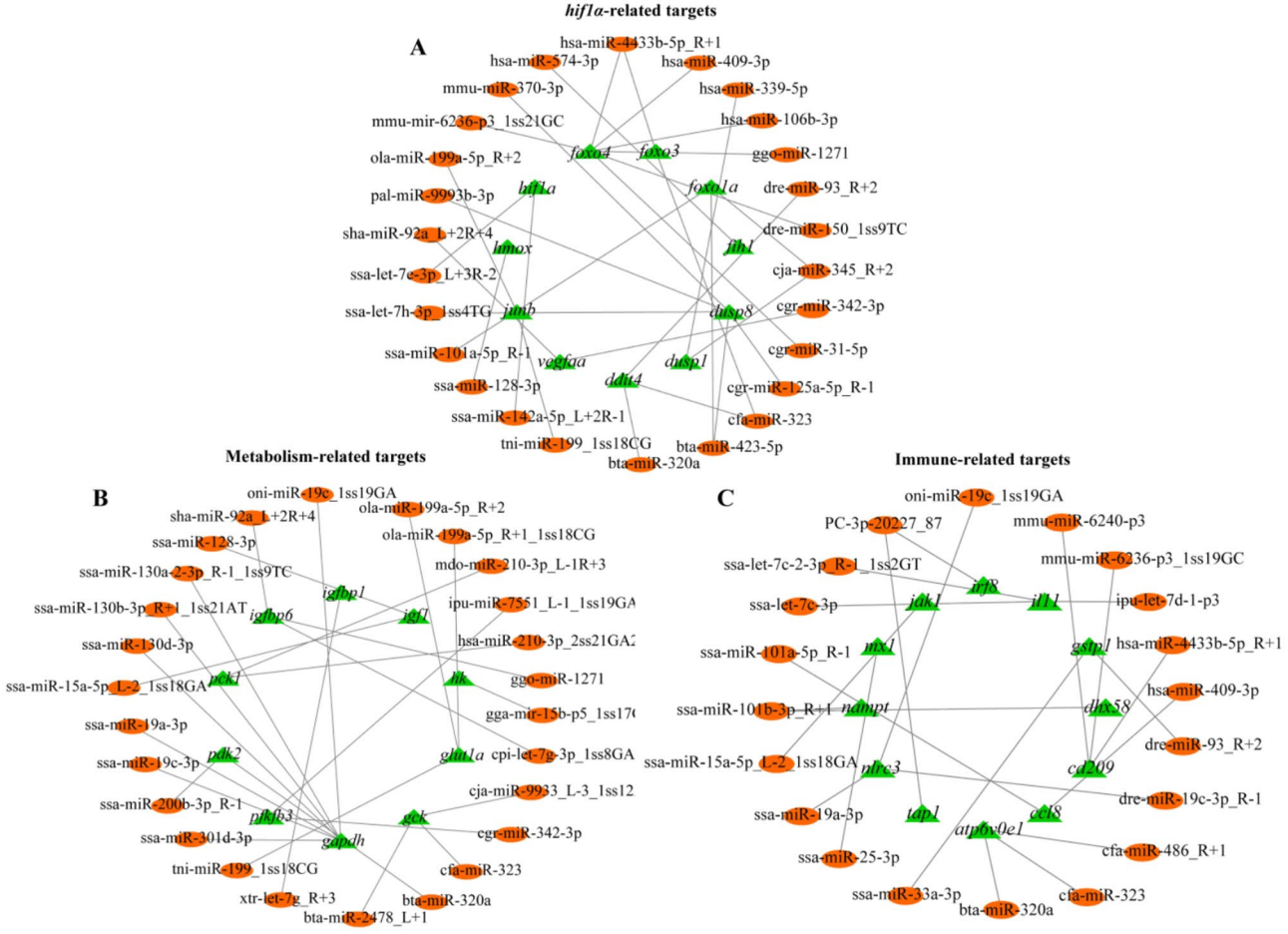

Fig. 3 Hypoxia-related miRNA-mRNA regulatory networks. **(A)** MiRNA targets related to *hif1a*. **(B)** MiRNA targets related to metabolism. **(C)** MiRNA targets related to immune response

Table 2 Key functional interaction pairs in rainbow trout under hypoxia and reoxygenation stress

miRNA name	Sequence (5′ to 3′)	Log_2 (fc)	*p*-value	Target gene
sha-miR-92a_L+2R+4	AATATTGCACTTGTCCCGGCCTGT	-1.34	2.47×10^{-3}	*vegfaa/igfbp6*
cgr-miR-342-3p	TCTCACACAGAAATCGCACCCGTC	-2.43	3.89×10^{-2}	*vegfaa/pfkfb3*
bta-miR-320a	AAAAGCTGGGTTGAGAGGGCGA	3.81	4.08×10^{-2}	*ddit4/pdk2*
cja-miR-345_R+2	GCTGACTCCTAGTCCAGGGCTC	-3.55	4.52×10^{-2}	*foxo1a/dusp1*
ssa-miR-128-3p	TCACAGTGAACCGGTCTCTTT	1.07	2.44×10^{-2}	*ho/igf1*
ssa-miR-101b-3p_R+1	TACAGTACTATGATAACTGAAG	3.54	2.21×10^{-2}	*igf1/dhx58/nampt*
ola-miR-199a-5p_R+2	CCCAGTGTTCAGACTACCTGTTCC	-2.39	3.98×10^{-2}	*junb/glut1a*
tni-miR-199_1ss18CG	CCCAGTGTTCAGACTACGTGTTC	-4.53	3.28×10^{-2}	*junb/glut1a*
bta-miR-423-5p	TGAGGGGCAGAGAGCGAGACTTT	-3.23	3.45×10^{-2}	*foxo1a/dusp8*
cfa-miR-323	CACATTACACGGTCGACCTCT	-5.34	2.23×10^{-2}	*foxo3/ddit4/gck*

of target genes of DE miRNAs. The results showed that ten significantly enriched pathways were identified in the H3h_L vs. N_L comparison (q-value < 0.05), including fatty acid metabolism, JAK-STAT signaling pathway, p53 signaling pathway, glycerophospholipid metabolism and AMPK signaling pathway (Table S5, Fig. 5A). Between the H12h_L and N_L groups, there were 39 significantly enriched pathways (q-value < 0.05), and lots of target genes were annotated to FoxO signaling pathway, mTOR signaling pathway, HIF-1 signaling pathway, insulin signaling pathway, AMPK signaling pathway, VEGF signaling pathway and p53 signaling pathway (Table S5, Fig. 5B). In the H24h_L vs. N_L comparison, a total of 38 pathways were enriched with q-value < 0.05, and top 15 pathways were mainly concentrated in metabolism, such as metabolism of xenobiotics by cytochrome P450, glycine, serine and threonine metabolism, arginine and proline metabolism, fatty acid metabolism, steroid hormone

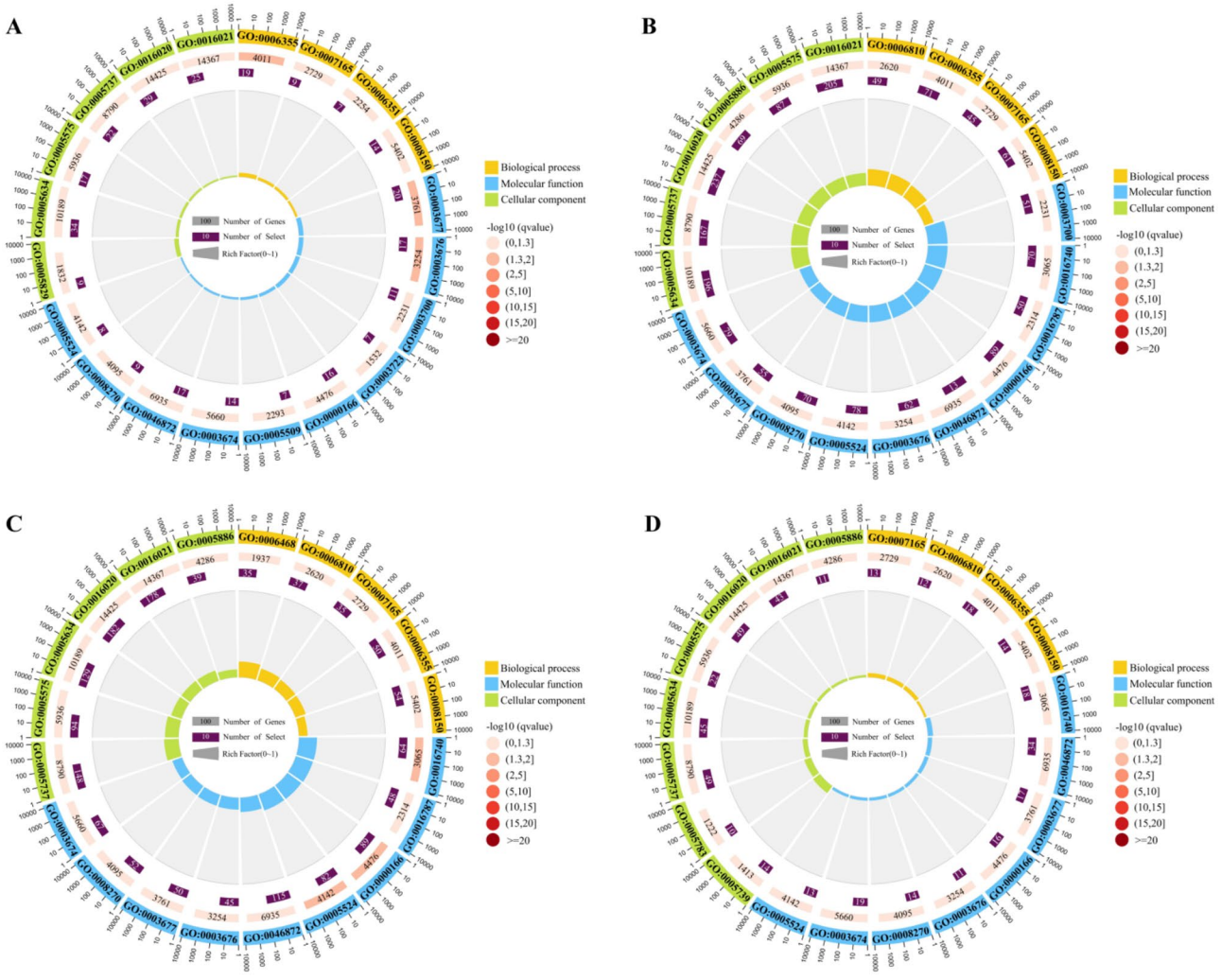

Fig. 4 GO enrichment analysis of target genes of DE miRNAs. **(A)** H3h_L vs. N_L. **(B)** H12h_L vs. N_L. **(C)** H24h_L vs. N_L. **(D)** R3h_L vs. N_L

biosynthesis; besides, 25 target genes were found to be involved in FoxO signaling pathway (Table S5, Fig. 5C). In the R3h_L vs. N_L comparison, six significantly enriched pathways, namely oxidative phosphorylation, protein processing in endoplasmic reticulum, viral carcinogenesis, phenylalanine metabolism, metabolism of xenobiotics by cytochrome P450 and phenylalanine, tyrosine and tryptophan biosynthesis were detected (q-value<0.05) (Table S5, Fig. 5D).

Co-expression network construction and key miRNAs screening using WGCNA

WGCNA is a powerful tool for identifying the sets of genes that are linked to phenotypes. As shown in Fig. 6A–C, three modules were obtained in 15 samples: turquoise (145 miRNAs), blue (80 miRNAs) and grey (four miRNAs), and the module expression patterns were visualized by the heatmaps and the module eigengene histograms (Fig. 6D and E). The results showed that the turquoise (R=0.72, p=1.9e-24) and blue (R=0.74, p=4.4e-15) modules were significantly correlated with hypoxia, which was consistent with the results of module–trait relationships analysis, but no correlation was found for the grey (R=0.85, p=0.068) module. After analysis, five key miRNAs with MM>0.8 and GS>0.2 were identified, including sha-miR-92a_L+2R+4, ssa-miR-128-3p, ssa-miR-101b-3p_R+1, ola-miR-199a-5p_R+2 and tni-miR-199_1ss18CG.

Validation of DE miRNAs by using RT-qPCR

RT-qPCR was performed on 14 DE miRNAs to confirm the results of miRNA-seq in the present study. As shown in Fig. 7, the variation trends of those miRNAs were consistent in both methods, which indicated that the miRNA-seq data were highly reliable.

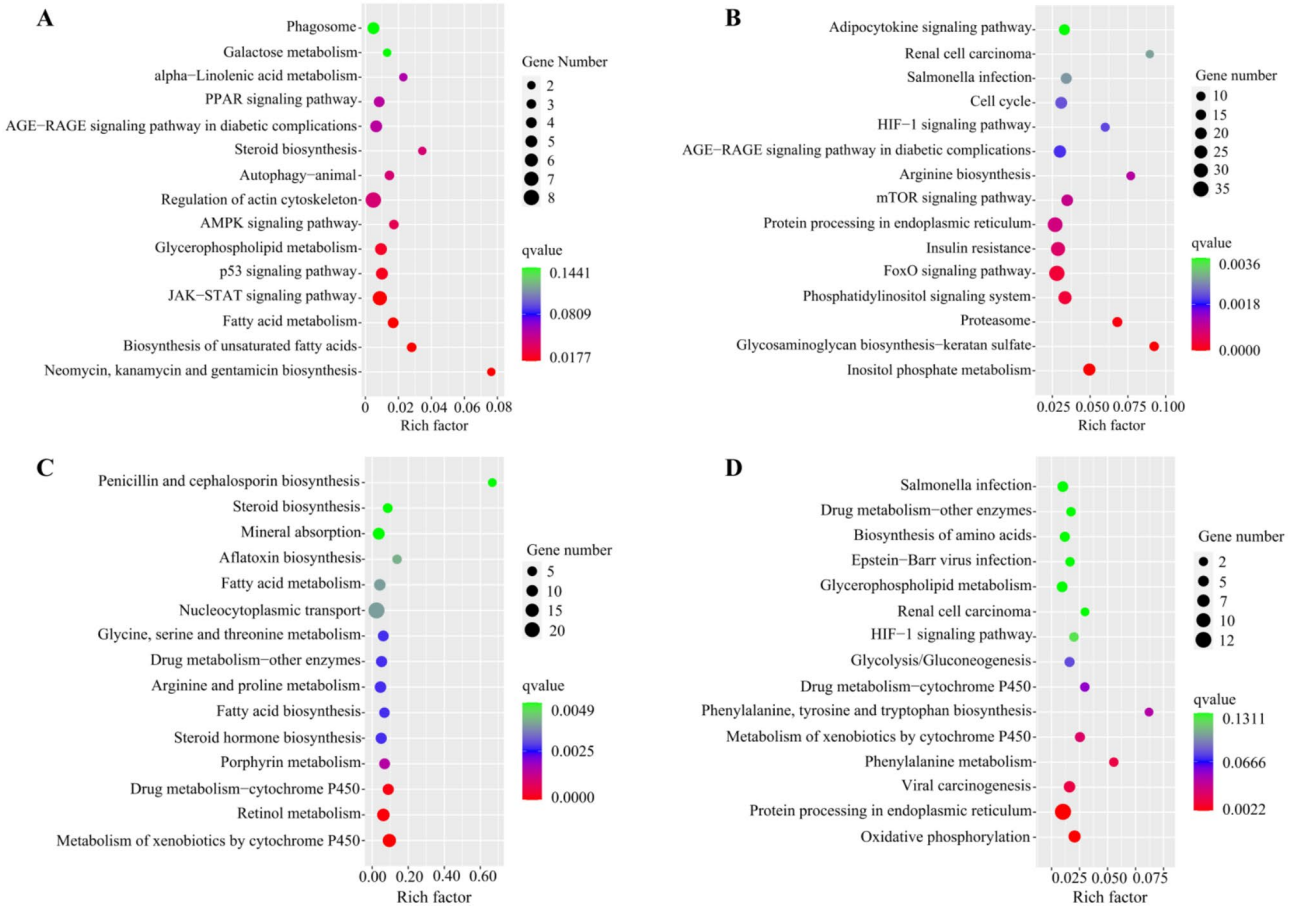

Fig. 5 The top 15 enriched KEGG pathways of target genes of DE miRNAs. **(A)** H3h_L vs. N_L. **(B)** H12h_L vs. N_L. **(C)** H24h_L vs. N_L. **(D)** R3h_L vs. N_L

Vegfaa was a target gene of sha-miR-92a_L+2R+4

Based on the bioinformatics analysis, the potential binding site between *vegfaa* and sha-miR-92a_L+2R+4 was identified (Fig. 8A). Luciferase assays showed that sha-miR-92a_L+2R+4 could inhibit the luciferase activity of *vegfaa*-wt, but it had no effect on the *vegfaa*-mut (Fig. 8B), suggesting *vegfaa* was a direct target of sha-miR-92a_L+2R+4.

Sha-miR-92a_L+2R+4 downregulated the expression level of *vegfaa*

During hypoxia stress and reoxygenation, we found that the expression of *vegfaa* was highest at H12h_L and lowest at H3h_L. Conversely, the expression of sha-miR-92a_L+2R+4 was highest at H3h_L and lowest at H12h_L (Fig. 8C and D). To investigate whether sha-miR-92a_L+2R+4 can regulate *vegfaa* expression, we overexpressed and inhibited sha-miR-92a_L+2R+4, respectively. The results revealed that sha-miR-92a_L+2R+4 mimics substantially decreased the expression level of *vegfaa* in rainbow trout liver cells, while the opposite results were obtained after transfection with sha-miR-92a_L+2R+4 inhibitor (Fig. 8E and F). These data suggested that there was a negative regulatory relationship between sha-miR-92a_L+2R+4 and *vegfaa*.

Sha-miR-92a_L+2R+4 promoted cell proliferation and inhibited apoptosis

To further explore the functions of sha-miR-92a_L+2R+4, the effects of sha-miR-92a_L+2R+4 on rainbow trout liver cell proliferation and apoptosis were detected. As shown in Fig. 9, sha-miR-92a_L+2R+4 overexpression promoted the cell viability and the percentage of EdU-positive cells compared with mimics NC group, and lower cell viability and fewer EdU-positive cells were found in the group with decreased sha-miR-92a_L+2R+4 expression compared with inhibitor NC group. In addition, we observed that overexpression of sha-miR-92a_L+2R+4 remarkably inhibited apoptosis, while apoptosis rate drastically elevated after sha-miR-92a_L+2R+4 inhibition compared with the respective control group (Fig. 10). The above results indicated that sha-miR-92a_L+2R+4 overexpression could promote cell proliferation and inhibit apoptosis.

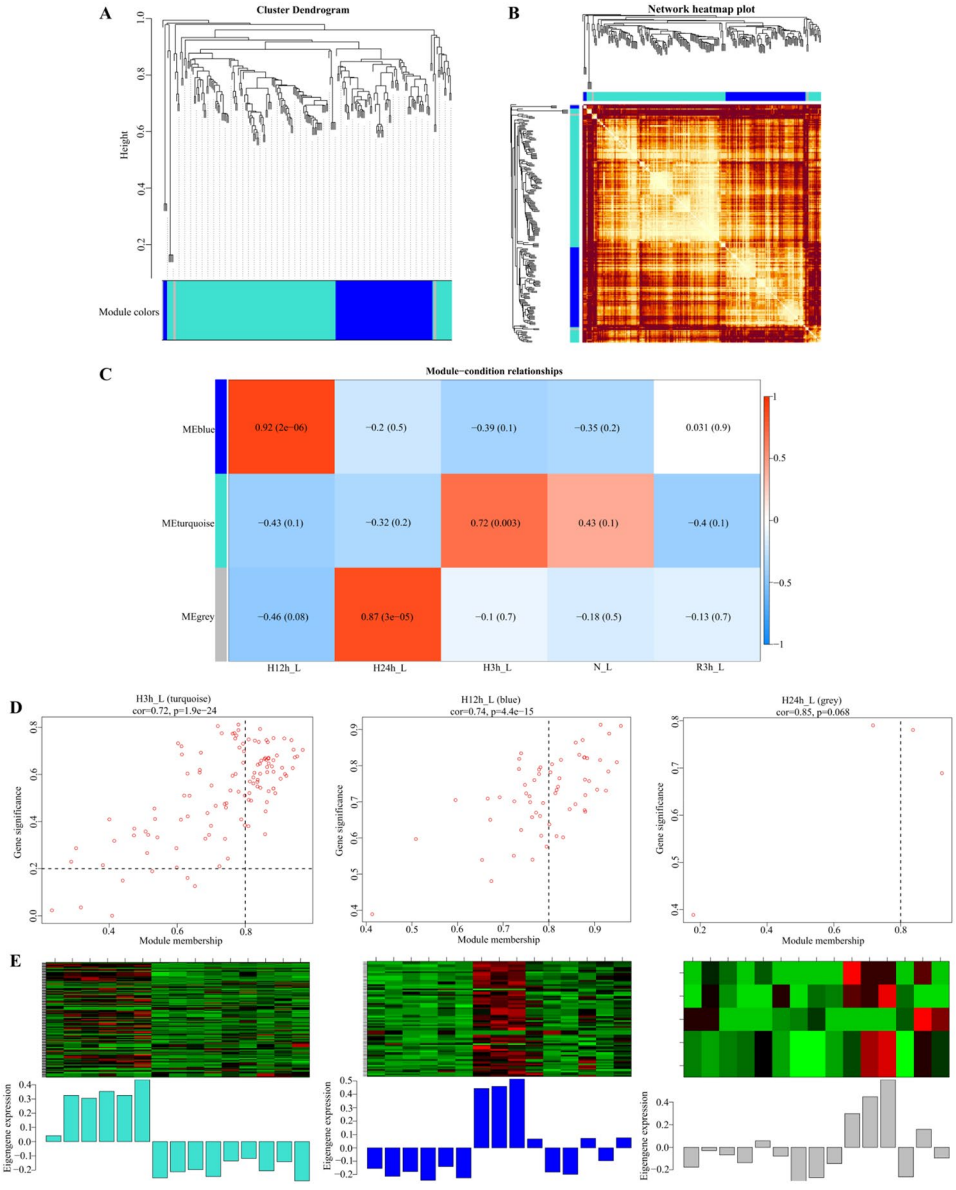

Fig. 6 WGCNA co-expression network and module-trait correlation analysis. **(A)** Cluster dendrogram of DE miRNAs. **(B)** Network heatmap plot of DE miRNAs. **(C)** Correlations of modules with traits. **(D)** The value distributions of module membership and gene significance of each miRNA in three modules. **(E)** Heatmaps of miRNA expression patterns in three modules

Discussion

Due to the increase in farming density and ecological deterioration, hypoxia has become one of the most critical environmental stressors causing a great loss of aquaculture [26]. As an economically important fish worldwide, rainbow trout has always been considered as a hypoxia-sensitive species, thus elucidation the molecular mechanisms in response to hypoxia is urgently needed [1]. Currently, despite a growing body of evidence has demonstrated that miRNAs with variable expression levels play essential roles in the adaptation of fish to hypoxia stress, few studies were performed to discuss the roles of miRNAs in rainbow trout under hypoxia stress [27]. Here, we described the miRNA profile changes under hypoxia for different durations and reoxygenation stress in rainbow trout, and functions of sha-miR-92a_L+2R+4 were investigated. The findings not only broaden our understanding of the regulatory roles of miRNAs under hypoxia stress in rainbow trout, but of practical importance in breeding hypoxia-tolerant rainbow trout.

MiRNAs are quite sensitive to external environmental changes and are treated as outposts of the cellular stress response [28]. In largemouth bass (*Micropterus salmoides*) and blunt snout bream (*Megalobrama amblycephala*), 84 and 132 miRNAs were detected as showing differential expression levels under hypoxia stress [27,

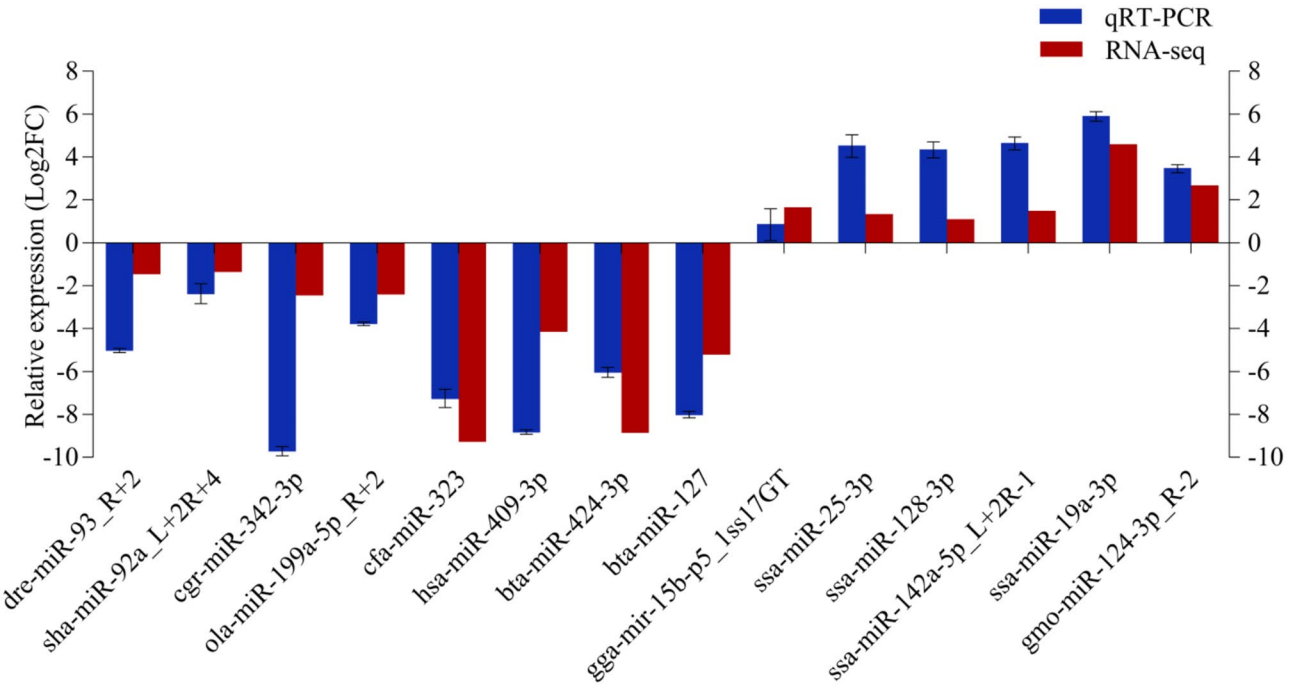

Fig. 7 Validation of miRNA-seq data of 14 DE miRNAs by RT-qPCR. Error bars indicate standard deviation of three replicates. Fold change of RT-qPCR result is expressed as the ratio of miRNA expression in challenged group (H3h_L, H12h_L, H24h_L or R3h_L) compared to that in N_L after normalization to U6

29]. In this study, a total of 192 DE miRNAs were identified by comparison of four treatment groups and control, suggesting miRNAs expression levels were altered to cope with the hypoxia response. Since DO is easily affected by natural perturbation, hypoxia stress in rainbow trout caused by abiotic factor such as temperature and climate may also yield similar results to those of the present experiments. After bioinformatics analysis, we obtained thousands of negative miRNA-mRNA pairs, which offer basic data for subsequent research and further provide a useful resource for rainbow trout genetics and breeding.

MiRNAs exert multiple biological functions through regulating the expression of target genes [30], and KEGG pathway analysis showed that many of DE miRNA targets in our results were significantly enriched in HIF-1 signaling pathway, which is essential for maintaining oxygen homeostasis [31]. *hif1α* serves as a master regulator of the response to hypoxia, and it becomes stable under hypoxic conditions and initiates more than 100 downstream genes transcription that participate in hypoxia adaptation, including *vegf* and *ho* [32, 33]. The activation of *vegf* and *ho* is a key step in the angiogenic response and defense against cellular injury under hypoxia [34, 35]. Previous studies have demonstrated that miR-462/miR-731, miR-204 and miR-155/miR-181a can directly target *hif1α*, *vegf* and *ho*, respectively [17, 18, 36]. Inconsistent with these results, we found that *hif1α*, *vegfaa* and *ho* were targeted by other miRNAs at H12h_L and H24h_L, such as ssa-let-7e-3p_L+3R-2, sha-miR-92a_L+2R+4, ssa-miR-142a-5p_L+2R-1, cgr-miR-342-3p, and ssa-miR-128-3p. This inconsistent targeting relationships reflected species-specificity and divergent evolution of miRNAs in different lineages. The results also indicated the critical roles of these miRNAs in hypoxia stress in rainbow trout. We further verified that *vegfaa* was a target of sha-miR-92a_L+2R+4, and there was a negative regulatory relationship between sha-miR-92a_L+2R+4 and *vegfaa*, suggesting the downregulation of sha-miR-92a_L+2R+4 expression under hypoxia stress contributes to angiogenesis, and this result can provide a potential basis for using miRNAs as target drugs to anti-hypoxia stress. In addition, miRNAs perform a crucial role in cell proliferation and apoptosis. Yu et al. [37] found that miR-92a-3p deletion inhibited breast cancer proliferation. Zheng et al., [38] found that low expression of miR-92a could promote prostate cancer cell apoptosis. Consistent with these studies, overexpression of sha-miR-92a_L+2R+4 promoted rainbow trout liver cell proliferation and suppressed apoptosis. Our finding indicated that hypoxia stress downregulated the expression of sha-miR-92a_L+2R+4, resulting in liver injury and liver cell apoptosis. Interestingly, the miRNAs targeting *hif1α* exhibited contrasting expression patterns in rainbow trout when compared to other species. The expression levels of let-7e and miR-142a were reported to decrease significantly in cobia and zebrafish under hypoxia stress [15, 39]. Here, apparent up-regulation of ssa-let-7e-3p_L+3R-2 and

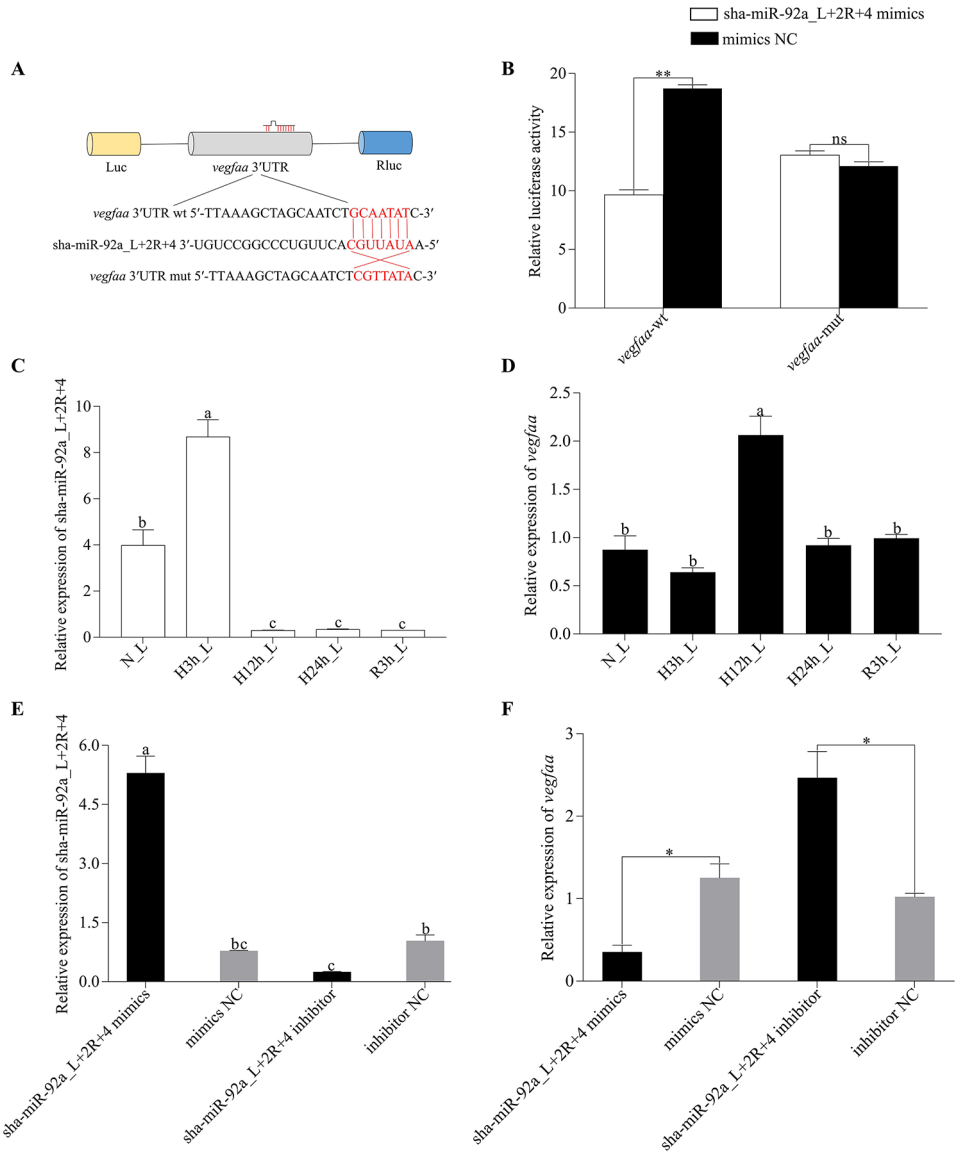

Fig. 8 sha-miR-92a_L+2R+4 targeted *vegfaa*. **(A)** The binding site of sha-miR-92a_L+2R+4 and *vegfaa*. **(B)** Relative luciferase activity in HEK293T cells cotransfected with *vegfaa*-wt/*vegfaa*-mut and sha-miR-92a_L+2R+4 mimics/mimics NC. **(C** and **D)** Relative expression of sha-miR-92a_L+2R+4 and *vegfaa* under hypoxia stress for different durations and reoxygenation. **(E and F)** sha-miR-92a_L+2R+4 and *vegfaa* expression in rainbow trout liver cells after transfection with sha-miR-92a_L+2R+4 mimics and inhibitor. Different letters above the bar represent significant differences. *: $P<0.05$; **: $P<0.01$; ns: $P>0.05$

ssa-miR-142a-5p_L+2R-1 and down-regulation of *hif1α* was found at H12h_L. This may be a pivotal reason why the hypoxia tolerance of rainbow trout is not as strong as that of other fish species.

Hypoxia and re-oxygenation can induce oxidative stress owing to the overproduction of reactive oxygen species (ROS), resulting in the damage of critical cellular macromolecules [40]. Studies have shown that miR-339-5p could suppress the antioxidant system by reducing superoxide dismutase (SOD), glutathione peroxidase (GSH-Px) and total antioxidant capacity (T-AOC) activities, and the inhibition of miR-31-5p attenuated oxidative stress [41, 42]; in contrast, miR-323-3p overexpression could enhance SOD activity to achieve relief from oxidative stress [43]. From our results, hsa-miR-339-5p, cfa-miR-323 and cgr-miR-31-5p were predicted to be involved in MAPK and FoxO signaling pathways with oxidative stress resistance function by regulating the expression of *dusp1*, *foxo3*/*ddit4* and *foxo4*, respectively. As well-known members of the MAPK and FoxO signaling pathways, up-regulation of *dusp1*, *foxo3* and *foxo4* was proven to increase the expression and activity of manganese superoxide dismutase (MnSOD) that can turn superoxide anion into comparatively less reactive

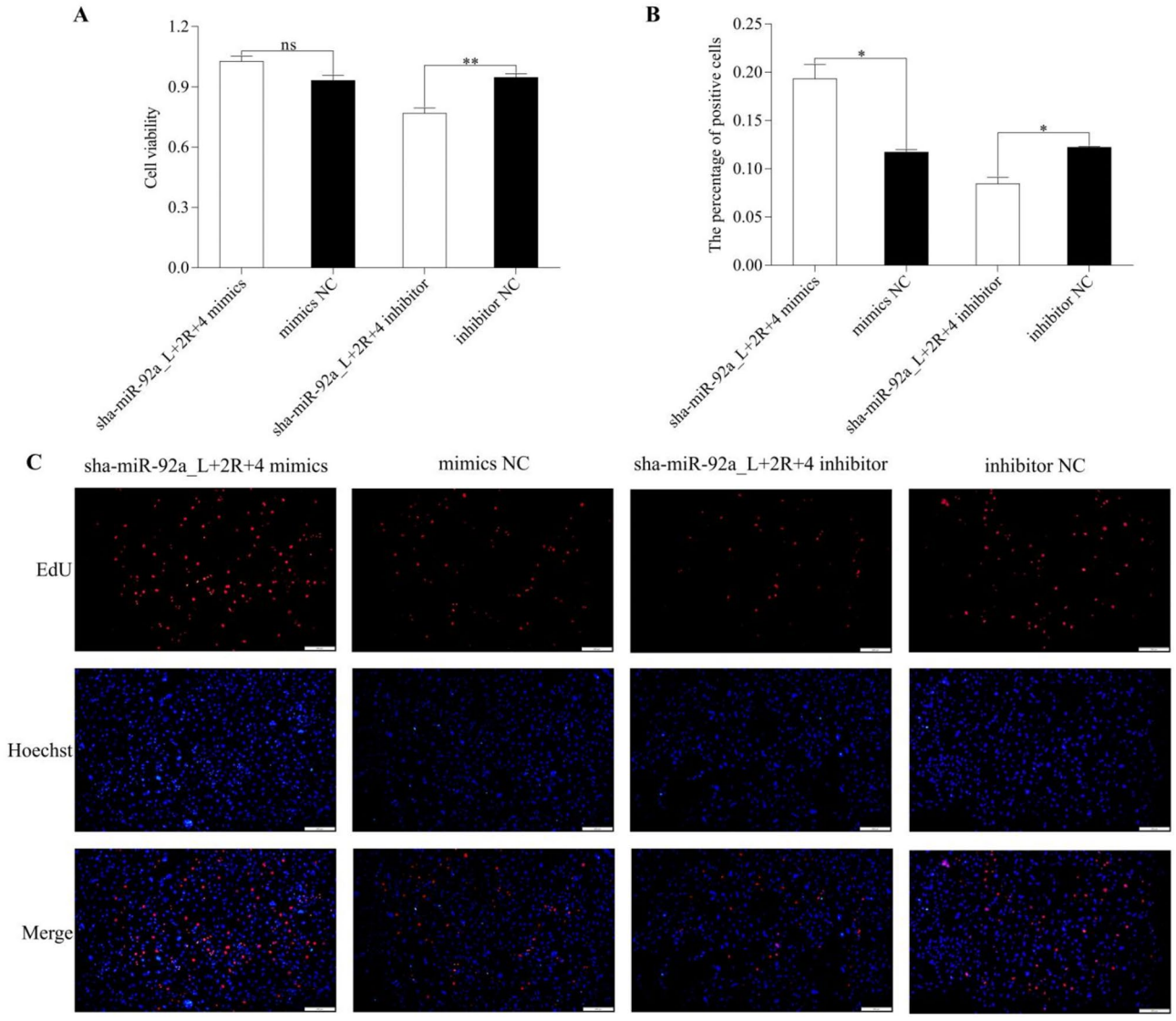

Fig. 9 Overexpression of sha-miR-92a_L + 2R + 4 promoted rainbow trout liver cell proliferation. **(A)** Changes in cell viability after transfected with sha-miR-92a_L + 2R + 4 mimics and inhibitor. **(B** and **C)** The effect of sha-miR-92a_L + 2R + 4 on cell proliferation was assessed by an EdU assay. *: $P < 0.05$; **: $P < 0.01$; ns: $P > 0.05$

hydrogen superoxide via cooperating with other antioxidant enzymes [44, 45]. *ddit4*, a negative regulator of the serine/threonine protein kinase mammalian target of rapamycin (mTOR) signaling pathway, has the effect of reducing ROS production [46]. These reports and our present results suggested that the significant down-regulation of hsa-miR-339-5p, cfa-miR-323 and cgr-miR-31-5p is conductive to timely scavenging ROS under hypoxia stress in rainbow trout, which contribute to the development of effective strategies for minimizing hypoxia caused damage in rainbow trout farming. Additionally, *fih1* and *junb* were predicted to be targeted separately by hsa-miR-574-3p and ola-miR-199a-5p_R + 2/tni-miR-199_1ss18CG. In rat (*Rattus norvegicus*), the regulatory relationship between miR-199a-5p and *junb* has been verified [47], which reflected the accuracy of targeting information obtained in this study. Besides *foxo3* and *foxo4*, *fih1* also functions as *hif1α* inhibitor, and the accumulation of FIH1 facilitates the degradation of HIF1α under hypoxia [48]. *junb* can act independently of HIF for maximal transcriptional induction of *vegf* [49]. It was thus clear that both down-regulated expression of ola-miR-199a-5p_R + 2 and tni-miR-199_1ss18CG promoted *vegfaa* expression to some extent. This could explain the opposite expression patterns of miRNAs targeting *hif1α* and *vegf* under hypoxia stress in rainbow trout.

In the face of hypoxic conditions, the metabolic transition from aerobic metabolism to anaerobic metabolism is an effective strategy for fish to promote hypoxia

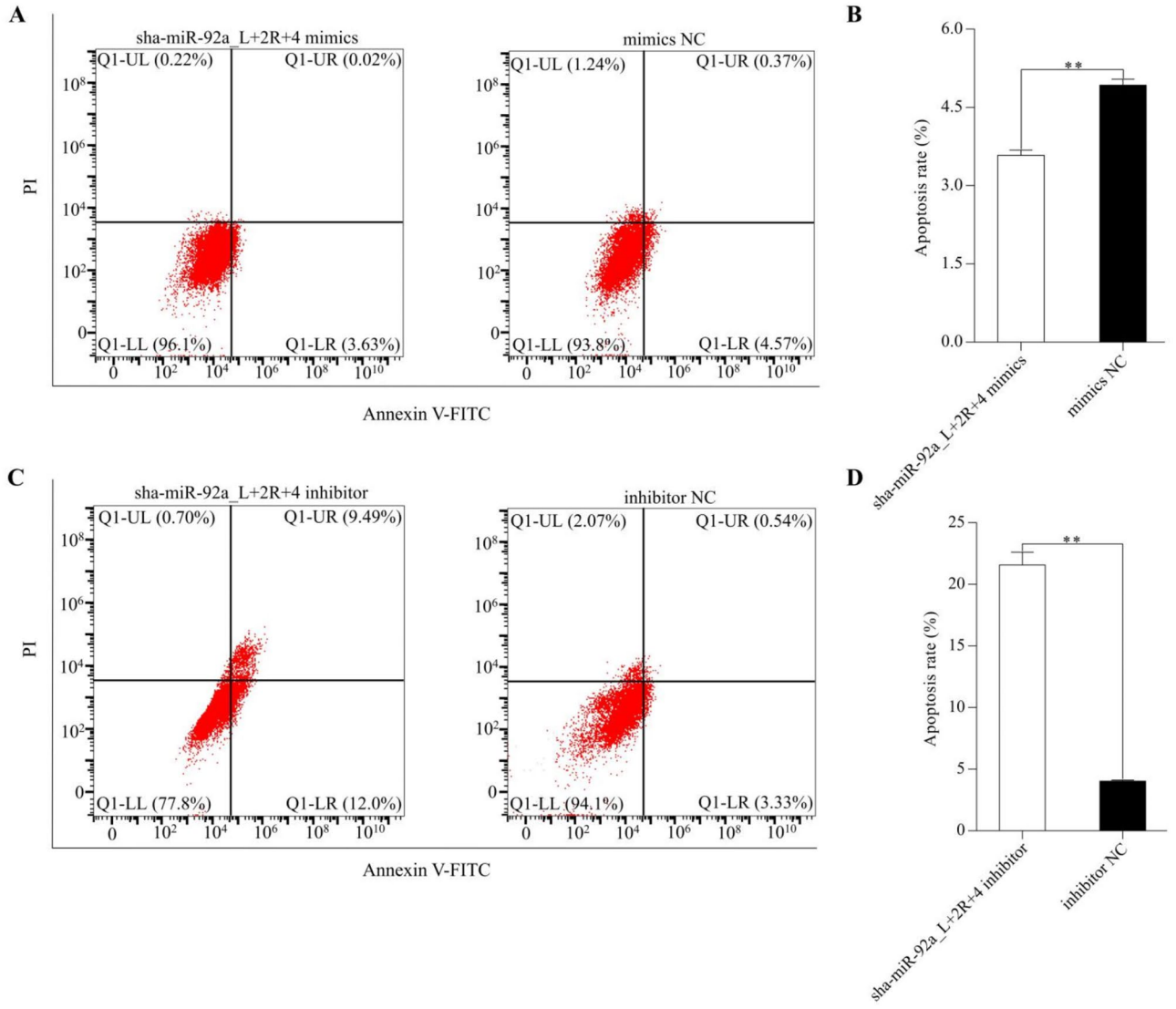

Fig. 10 Overexpression of sha-miR-92a_L + 2R + 4 inhibited apoptosis. **(A** and **B)** The apoptosis rates after transfected with sha-miR-92a_L + 2R + 4 mimics and mimic NC. **(C** and **D)** The apoptosis rates after transfected with sha-miR-92a_L + 2R + 4 inhibitor and inhibitor NC. Apoptosis rate indicates the sum of early and late apoptotic cell ratio (Q1-LR + Q1-UR). *: $P < 0.05$; **: $P < 0.01$; ns: $P > 0.05$

adaptation [50]. In the study of Atlantic cod (*Gadus morhua*), it was observed that the target gene of miR-143 was hexokinase (*hk*), which can accelerate glycolysis and produce ATP under hypoxic environments [51]. Qiang et al. [10] reported that miR-34a could directly target *glut1* to mediate the glycolytic pathway under hypoxia stress in tilapia. According to enrichment analysis, it is worth noting that hundreds of target genes of DE miRNAs fell into metabolic processes GO term, and glycolysis/gluconeogenesis, fatty acid metabolism, porphyrin metabolism, and arginine and proline metabolism KEGG pathways. Among these, we found that *glut1a*, glucokinase (*gck*), glyceraldehyde-3-phosphate dehydrogenase (*gapdh*), pyruvate dehydrogenase kinase 2 (*pdk2*) and 6-phosphofructo-2-kinase (*pfkfb3*) were targeted by numerous miRNAs, including ola-miR-199a-5p_R + 2, cfa-miR-323, ssa-miR-19a-3p, bta-miR-320a and cgr-miR-342-3p, implying these miRNAs perform a crucial role in a rapid adaptive activation of anaerobic ATP-generating pathway. Furthermore, phosphoenolpyruvate carboxykinase (*pck1*) was predicted to be targeted by mdo-miR-210-3p_L-1R + 3. MiR-210-3p was observed to be up-regulated in rainbow trout epidermal mucus under hypoxia stress [52]. In this study, the down-regulation of mdo-miR-210-3p_L-1R + 3 in liver induced by hypoxia indicated that its expression is tissue specific. *pck1*, a key rate-limiting enzyme that initiates gluconeogenesis, is considered indispensable for glucose homeostasis [53]. The down-regulation of mdo-miR-210-3p_L-1R + 3 may

facilitate the activation of the gluconeogenic pathway and increase generation of glucose and glycogen.

Except for the above DE miRNAs, other miRNAs with high expression levels were found to target several key immune-related genes. For instances, toll-like receptor 3 (*tlr3*) and myxovirus resistance-1 (*mx1*) were targeted by ssa-miR-25-3p, DEXH (Asp-Glu-X-His) box polypeptide 58 (*dhx58*) was targeted by ssa-miR-101b-3p_R+1, and C-C motif chemokine 8 (*ccl8*) was targeted by hsa-miR-409-3p. In mice (*Mus musculus*), miR-25-3p and miR-409-3p expression was considered to be induced by inflammatory mediators, and it can stimulate secretion of pro-inflammatory cytokines, such as tumor necrosis factor-alpha (*tnf-α*), interleukin-1α (*il-1α*), *il-1β*, *il-6* and *il-17* [54, 55]. MiR-101b-3p is known to regulate Wnt signaling pathway and proliferation of muscle cells in crisp grass carp (*Ctenopharyngodon idellus* C. et V.) [56]. *mx1* has been shown to exert anti-viral actions against a broad range of RNA viruses in fish, and up-regulation of *dhx58* and *tlr3* contributed to the transcriptional activation of *mx1* via triggering JAK-STAT signaling pathway [57, 58]. Hence, the significant up-regulation of ssa-miR-25-3p and ssa-miR-101b-3p_R+1 suggested that rainbow trout is less resistant to viruses under hypoxia stress. We also found that glutathione S-transferase P1 (*gstp1*) associated with the metabolism of xenobiotics by cytochrome P450 was targeted by ssa-miR-33a-3p and dre-miR-93_R+2. Usually, *gstp1* expression is induced by xenobiotics, and inflammatory cytokines can reduce the generation of highly immunotoxic metabolites derived from xenobiotics by inhibiting cytochrome P450 enzymes activities in fish [59, 60]. Taken together, these results showed that ssa-miR-33a-3p and dre-miR-93_R+2 together with miR-25-3p and miR-409-3p play an essential role in protecting rainbow trout from xenobiotics under hypoxia stress.

Conclusion

This study systematically investigated the potential roles of miRNAs in rainbow trout under hypoxia stress for different durations and reoxygenation stress. After miRNA-mRNA interaction analysis, dozens of hypoxia-responsive miRNAs were identified, and enrichment analyses showed that these miRNAs were involved in the regulation of HIF-1 signaling pathway, FoxO signaling pathway, VEGF signaling pathway, oxidative stress, energy metabolism and immune response. Further research found that sha-miR-92a_L+2R+4 could directly regulate *vegfaa* expression, and overexpression of sha-miR-92a_L+2R+4 promoted liver cell proliferation and inhibited apoptosis. The results of this study provide significant clues for a better understanding of the crucial roles of miRNAs under hypoxia and reoxygenation stress, and provide useful resources for breeding hypoxia-tolerant rainbow trout.

Materials and methods

Hypoxia treatment and sample collection

The experimental rainbow trout (200±10.5 g) that belonged to a full-sib family were purchased from a fish farm in Yongjing, Gansu Province, China. Before the formal experiment, fifty healthy fish were maintained in a 300 L water tank for two weeks (DO=7.5±0.1 mg/L, water temperature=12±0.1 °C, pH=7.5±0.1) and fed with commercial pellet feed twice daily. After two weeks of temporary rearing, nitrogen was used to reduce the DO in water from 7.5±0.1 mg/L to 3.5±0.1 mg/L. Liver tissues of rainbow trout were collected after anesthetization by MS-222 (Sigma Aldrich Co., St. Louis, USA): control (DO=7.5±0.1 mg/L, N_L), hypoxia for 3 h (DO=3.5±0.1 mg/L, H3h_L), hypoxia for 12 h (DO=3.5±0.1 mg/L, H12h_L), hypoxia for 24 h (DO=3.5±0.1 mg/L, H24h_L) and normal oxygen recovered in 3 h after hypoxia 24 h (DO=7.5±0.1 mg/L, R3h_L). Each stage contained 10 individuals. After sampling, the samples were immediately frozen in liquid nitrogen and stored at −80 ℃ until processing. All experiments complied with institutional guidelines and the protocol was approved by the Animal Experimentation Ethics Committee at Gansu Agricultural University, China (GSAU-Eth-AST-2021-004).

RNA extraction, library construction and sequencing

Total RNA from 15 liver tissues was extracted using TRIzol reagent (Invitrogen, Carlsbad, CA, USA) following the manufacturer's protocols, and RNA integrity and quality were estimated with 1% agarose gel electrophoresis and Agilent 2100 Bioanalyzer (Agilent Technologies, Palo Alto, CA, USA). High-quality total RNA from each sample was used to constructed the cDNA libraries of miRNA using a TruSeq small RNA Sample Prep Kit (Illumina, San Diego, CA, USA) according to the manufacturer's recommendations. After the libraries' quality tests were passed, 15 libraries were sequenced on an Illumina Hiseq 2500, and 50 bp single-end reads were generated.

Data processing and screening of differentially expressed (DE) miRNAs

The raw reads contained adapter dimers, junk, low complexity, common RNA families (rRNA, tRNA, snRNA and snoRNA) and repeats were removed by ACGT101-miR (LC Sciences, Houston, Texas, USA). Subsequently, all retained reads were searched against the miRBase database (22.0) to identify known miRNAs, and unmapped sequences were blasted against reference genome to identify novel miRNAs according to their genome positions and hairpin structures through RNAfold software. DESeq2 (v.1.6.3) was used to analyze DE miRNAs with parameters of $|\text{Log}_2$ fold change$| > 1$ and p-value<0.05 [61], and DE miRNAs with similar

expression trends during the hypoxia and reoxygenation stress were clustered using STEM [62].

Target genes prediction of DE miRNAs and functional enrichment analysis

Combined with previously obtained transcriptome data [25], we used TargetScan (Version: 7.0) and miRanda (v3.3a) to predict the target genes for DE miRNAs, and data predicted by both algorithms were combined and the overlaps were calculated. Co-expressed negatively miRNA-mRNA pairs were identified based on the following thresholds: Pearson correlation coefficient (PCC) <-0.7 and p-value <0.05. The visualization of miRNA-mRNA regulatory network was performed by Cytoscape (v3.6.0).

To annotate the function of these DE miRNAs, the target genes of DE miRNAs were subjected to an enrichment analysis of GO and KEGG pathways. The terms or pathways with q-value <0.05 were considered to be significantly enriched.

Weighted gene co-expression network analysis (WGCNA)

To identify modules of co-expressed DE miRNAs associated with hypoxia stress, the TPM of all DE miRNAs in 15 samples was used for WGCNA. Modules with Pearson correlation coefficient >0.5 and $p<0.05$ were considered to be related to hypoxia exposure, and the criteria for filtering key miRNAs were module membership (MM) >0.8 and gene significance (GS) >0.2.

RT-qPCR validation

To validate the expression levels of DE miRNAs from miRNA-seq, 14 DE miRNAs were selected for RT-qPCR analysis (Table S1). The RNA used for Illumina sequencing was also used here for the validation. cDNA synthesis was conducted with the Mir-X miRNA First-Strand Synthesis Kit (Clontech, Mountain View, CA, USA). RT-qPCR was performed in accordance with the protocol provided by the SYBR Premix Ex Taq (Takara, China) on a LightCycler 480 II Instrument (Roche, Basel, Switzerland). The reaction system was 20 μL and contained 1.6 μL of cDNA, 0.4 μL of each sense and antisense primer (10 μM), 10 μL of SYBR Premix Ex Taq II (2×) and 7.6 μL of ddH_2O. The amplification program consisted of one cycle at 95 °C for 10 s, followed by 40 cycles of 95 °C for 5 s and 60 °C for 20 s. Melting curve analysis was carried out at the end of the RT-qPCR to determine the target specificity. U6 was used as the housekeeping gene, and relative expression levels of targets versus U6 were analyzed using the $2^{-\Delta\Delta Ct}$ method [63].

Dual-luciferase reporter assay

According to the binding site predicted by TargetScan (Version: 7.0) and miRanda (v3.3a), the wild-type *vegfaa*-3′-UTR (*vegfaa*-wt) and mutant *vegfaa*-3′-UTR (*vegfaa*-mut) were designed and then cloned into the pmirGLO vector. In 96-well plate, HEK293T cells were cultured to approximately 70% confluence, the plasmid was co-transfected with sha-miR-92a_L+2R+4 mimics or mimics negative control (NC) into HEK293T cells. After 48 h post-transfection, the cells were harvested and detected using Dual-Glo® Luciferase Assay System (Promega, USA) in line with the manufacturer's protocol. Finally, relative activity of fluorescein (Firefly luciferase activities/Renilla luciferase activities) was obtained through a microplate reader (Thermo, USA).

Over- and down-expression of sha-miR-92a_L+2R+4

Transfection was performed referring to previous report [64]. Briefly, sha-miR-92a_L+2R+4 mimics and sha-miR-92a_L+2R+4 inhibitor and their corresponding NC were synthesized by Genepharma Co. Ltd (Shanhai, China) (Table S1). For transfection, the rainbow trout liver cells were transfected at 80% confluence with sha-miR-92a_L+2R+4 mimics, mimics NC, sha-miR-92a_L+2R+4 inhibitor and inhibitor NC using NVI DNA RNA transfection reagent (Invigentech, USA), following the instructions of manufacturer. After transfected for 48 h, the cells were collected and then used for expression analysis.

Cell viability and EdU staining assay

Cell viability was determined using a Cell Counting Kit-8 (CCK-8, Solarbio, China) in accordance with the manufacturer's instructions. For the CCK-8 assay, rainbow trout liver cells were seeded in a 96-well plate and were transiently transfected with sha-miR-92a_L+2R+4 mimics, sha-miR-92a_L+2R+4 inhibitor and their NC for 48 h. Then, 10 μL of CCK-8 solution was added into each well, and the plate was left at 20 ℃ for additional 2 h. Following that, the values of optical density were analyzed at 450 nm using a microplate reader.

Next, EdU staining was used to analyze the effect of on rainbow trout liver cells proliferation according to the manufacturer's procedures of the BeyoClick™ EdU Cell Proliferation Kit with Alexa Fluor 555 (Beyotime, China). After transfection, the liver cells in each well were incubated with 500 μL of EdU (20 μM) for 24 h at 20 ℃, and subsequently fixed with 4% paraformaldehyde for 30 min. 100 μL of click reaction buffer was added to culture medium, and incubating the cells at room temperature in dark for 30 min. Afterwards, the nuclei stained with Hoechst dye 33,342 were observed by fluorescence microscope (Olympus IX71, Japan).

Flow cytometry assay

Apoptosis was evaluated with an Apoptosis and Necrosis Assay Kit (Beyotime, China). After transfected with sha-miR-92a_L+2R+4 mimics, sha-miR-92a_L+2R+4 inhibitor and their NC for 48 h in 6-well plate, the liver

cells were harvested, and cell suspension was treated with 5 μL annexin V-FITC followed by 5 μL propidium iodide in dark and incubated for 10–15 min at 4 °C. The percentage of apoptosis in different treatment groups was measured by flow cytometry (Beckman, USA).

Abbreviations

DE	Differentially expressed
DO	Dissolved oxygen
UTR	Untranslated region
GO	Gene Ontology
KEGG	Kyoto Encyclopedia of Genes and Genomes
PCC	Pearson correlation coefficient
GS	Gene significance

Supplementary Information

The online version contains supplementary material available at https://doi.org/10.1186/s12864-024-11019-1.

Supplementary Material 1: Fig. S1. Pearson's correlation coefficients between samples. Table S1. The sequence of primers used in this study. Table S2. DE miRNAs between the four treatment groups and the normoxia. Table S3. Negatively correlated miRNA-mRNA pairs between the four treatment groups and the normoxia. Table S4. GO enrichment analysis of targets of DE miRNAs between the four treatment groups and the normoxia. Table S5. KEGG enrichment analysis of targets of DE miRNAs between the four treatment groups and the normoxia.

Acknowledgements

We gratefully acknowledge the assistance of Tongzhen Sun with fish rearing and tissue sampling.

Author contributions

YJL: Writing–original draft, formal analysis and project administration; SJW: Data curation and validation; JQH: Conceptualization and writing–review & editing; LZ: Investigation. All authors read and approved the final manuscript.

Funding

This research was supported by the National Natural Science Foundation of China (Grant No. 32060823), Fostering Foundation for the Excellent Ph.D. Dissertation of Gansu Agricultural University (YB2022001) and Discipline Team Project of Gansu Agricultural University (GAU-XKTD-2022-23).

Data availability

Sequence data that support the findings of this study have been deposited in the National Center for Biotechnology Information (NCBI) database (GSE231752).

Declarations

Ethics approval and consent to participate

The animal study was reviewed and approved by the Faculty Animal Policy and Welfare Committee of Gansu Agricultural University (Lanzhou, China; Ethic approval file No. GSAU-Eth-AST-2021-004). All experimental procedures and sample collection methods were performed in accordance with approved guidelines and regulations to ensure animal welfare. Meanwhile, the study is in accordance with ARRIVE guidelines.

Consent for publication

Not applicable.

Competing interests

The authors declare no competing interests.

Received: 8 January 2024 / Accepted: 8 November 2024
Published online: 02 December 2024

References

1. Hou ZS, Wen HS, Li JF, He F, Li Y, Qi X. Environmental hypoxia causes growth retardation, osteoclast differentiation and calcium dyshomeostasis in juvenile rainbow trout (*Oncorhynchus mykiss*). Sci Total Environ. 2020;705:135272.
2. Wang SY, Lau K, Lai KP, Zhang JW, Tse AC, Li JW, et al. Hypoxia causes transgenerational impairments in reproduction of fish. Nat Commun. 2016;7:12114.
3. Ding J, Liu C, Luo S, Zhang Y, Gao X, Wu X, et al. Transcriptome and physiology analysis identify key metabolic changes in the liver of the large yellow croaker (*Larimichthys crocea*) in response to acute hypoxia. Ecotoxicol Environ Saf. 2020;189:109957.
4. Abdel-Tawwab M, Monier MN, Hoseinifar SH, Faggio C. Fish response to hypoxia stress: growth, physiological, and immunological biomarkers. Fish Physiol Biochem. 2019;45:997–1013.
5. Joyce W, Perry SF. Hypoxia inducible factor-1α knockout does not impair acute thermal tolerance or heat hardening in zebrafish. Biol Lett. 2020;16:20200292.
6. Dawood MAO, Noreldin AE, Sewilam H. Long term salinity disrupts the hepatic function, intestinal health, and gills antioxidative status in Nile tilapia stressed with hypoxia. Ecotoxicol Environ Saf. 2021;220:112412.
7. He J, Yu Y, Li ZM, Liu ZM, Weng SP, Guo CJ, et al. Hypoxia triggers the outbreak of infectious spleen and kidney necrosis virus disease through viral hypoxia response elements. Virulence. 2022;13:714–26.
8. Zhao SS, Su XL, Pan RJ, Lu LQ, Zheng GD, Zou SM. The transcriptomic responses of blunt snout bream (*Megalobrama amblycephala*) to acute hypoxia stress alone, and in combination with bortezomib. BMC Genomics. 2022;2:162.
9. Sun JL, Zhao LL, Wu H, Liu Q, Liao L, Luo J, et al. Acute hypoxia changes the mode of glucose and lipid utilization in the liver of the largemouth bass (*Micropterus salmoides*). Sci Total Environ. 2020;713:135157.
10. Qiang J, Zhu XW, He J, Tao YF, Bao JW, Zhu JH, et al. miR-34a regulates the activity of HIF-1a and P53 signaling pathways by promoting *GLUT1* in genetically improved farmed tilapia (GIFT, *Oreochromis niloticus*) under hypoxia stress. Front Physiol. 2020;11:670.
11. Saliminejad K, Khorram Khorshid HR, Soleymani Fard S, Ghaffari SH. An overview of microRNAs: Biology, functions, therapeutics, and analysis methods. J Cell Physiol. 2019;234:5451–65.
12. Tse AC, Li JW, Wang SY, Chan TF, Lai KP, Wu RS. Hypoxia alters testicular functions of marine medaka through microRNAs regulation. Aquat Toxicol. 2016;180:266–73.
13. Li J, Zhang G, Yin D, Li Y, Zhang Y, Cheng J, et al. Integrated application of multiomics strategies provides insights into the environmental hypoxia response in *Pelteobagrus vachelli* muscle. Mol Cell Proteom. 2022;21:100196.
14. Wang Q, Li X, Sha H, Luo X, Zou G, Liang H. Identification of microRNAs in silver carp (*Hypophthalmichthys molitrix*) response to hypoxia stress. Animals. 2021;11:2917.
15. Huang JS, Li HJ, Guo ZX, Zhang JD, Wang WZ, Wang ZL, et al. Identification and expression analysis of cobia (*Rachycentron canadum*) liver-related miRNAs under hypoxia stress. Fish Physiol Biochem. 2021;47:1951–67.
16. Li Y, Wu S, Huang J, Zhao L. Integration of physiological, miRNA-mRNA interaction and functional analysis reveals the molecular mechanism underlying hypoxia stress tolerance in crucian carp (*Carassius auratus*). FASEB J. 2024;38:e23722.
17. Zhao Y, Zhu CD, Yan B, Zhao JL, Wang ZH. miRNA-directed regulation of VEGF in tilapia under hypoxia condition. Biochem Biophys Res Commun. 2014;454:183–8.
18. Huang CX, Chen N, Wu XJ, Huang CH, He Y, Tang R, et al. The zebrafish miR-462/miR-731 cluster is induced under hypoxic stress via hypoxia-inducible factor 1α and functions in cellular adaptations. FASEB J. 2015;29:4901–13.
19. Wu S, Huang J, Li Y, Zhao L. Comparative transcriptomics combined with physiological and functional analysis reveals the regulatory mechanism of rainbow trout (*Oncorhynchus mykiss*) under acute hypoxia stress. Ecotoxicol Environ Saf. 2024;278:116347.
20. Wu S, Huang J, Li Y. A novel hypoxic lncRNA, LOC110520012 sponges mir-206-y to regulate angiogenesis and liver cell proliferation in rainbow trout (*Oncorhynchus mykiss*) by targeting *vegfaa*. Ecotoxicol Environ Saf. 2024;280:116554.
21. Wu S, Huang J, Li Y, Zhao L. Integrated physiological, whole transcriptomic and functional analysis reveals the regulatory mechanism in the liver of rainbow trout (*Oncorhynchus mykiss*) in response to short-term and chronic hypoxia stress. Aquaculture. 2024;593:741250.

22. Thurston RV, Phillips GR, Russo RC, Hinkins SM. Increased toxicity of ammonia to rainbow trout (*Salmo Gairdneri*) resulting from reduced concentrations of dissolved oxygen. Can J Fish Aquat Sci. 1981;38:983–8.
23. Baze MM, Schlauch K, Hayes JP. Gene expression of the liver in response to chronic hypoxia. Physiol Genomics. 2010;41:275–88.
24. Kang PM, Haunstetter A, Aoki H, Usheva A, Izumo S. Morphological and molecular characterization of adult cardiomyocyte apoptosis during hypoxia and reoxygenation. Circ Res. 2000;87:118–25.
25. Wu S, Huang J, Li Y, Pan Y. Dynamic and systemic regulatory mechanisms in rainbow trout (*Oncorhynchus mykiss*) in response to acute hypoxia and reoxygenation stress. Aquaculture. 2023;572:739540.
26. Shang FQ, Bao MX, Liu FJ, Hu ZW, Wang SN, Yang X. Transcriptome profiling of tiger pufferfish (*Takifugu rubripes*) gills in response to acute hypoxia. Aquaculture. 2022;557:738324.
27. Sun JL, Zhao LL, He K, Liu Q, Luo J, Zhang D, et al. MicroRNA regulation in hypoxic environments: differential expression of microRNAs in the liver of largemouth bass (*Micropterus salmoides*). Fish Physiol Biochem. 2020;46:2227–42.
28. Kim SB, Zhang L, Barron S, Shay JW. Inhibition of microRNA-31-5p protects human colonic epithelial cells against ionizing radiation. Life Sci Space Res (Amst). 2014;1:67–73.
29. Sun S, Xuan F, Ge X, Zhu J, Zhang W. Dynamic mRNA and miRNA expression analysis in response to hypoxia and reoxygenation in the blunt snout bream (*Megalobrama amblycephala*). Sci Rep. 2017;7:12846.
30. Bartel DP. MicroRNAs: target recognition and regulatory functions. Cell. 2009;136:215–33.
31. Macklin PS, McAuliffe J, Pugh CW, Yamamoto A. Hypoxia and HIF pathway in cancer and the placenta. Placenta. 2017;56:8–13.
32. Palazon A, Goldrath AW, Nizet V, Johnson RS. HIF transcription factors, inflammation, and immunity. Immunity. 2014;41:518–28.
33. Semenza GL. Hypoxia-inducible factor 1 (HIF-1) pathway. Sci STKE. 2007; 2007: cm8.
34. Kon M, Ikeda T, Homma T, Suzuki Y. Responses of angiogenic regulators to resistance exercise under systemic hypoxia. J Strength Cond Res. 2021;35:436–41.
35. Li Q, Dasari C, Li D, Arshia A, Umer AM, Abouzid MRA, et al. Effects of heme oxygenase-1 on c-kit-positive cardiac cells. Int J Mol Sci. 2021;22:13448.
36. Li H, Di G, Zhang Y, Xue R, Zhang J, Liang J. MicroRNA-155 and microRNA-181a, via *HO-1*, participate in regulating the immunotoxicity of cadmium in the kidneys of exposed *Cyprinus carpio*. Fish Shellfish Immunol. 2019;95:473–80.
37. Yu ZH, Chen ZH, Zhou GL, Zhou XJ, Ma HY, Yu Y, et al. miR-92a-3p promotes breast cancer proliferation by regulating the KLF2/BIRC5 axis. Thorac Cancer. 2022;13:2992–3000.
38. Yanshen Z, Lifen Y, Xilian W, Zhong D, Huihong M. miR-92a promotes proliferation and inhibits apoptosis of prostate cancer cells through the PTEN/Akt signaling pathway. Libyan J Med. 2021;16:1971837.
39. Luu I, Ikert H, Craig PM. Chronic exposure to anthropogenic and climate related stressors alters transcriptional responses in the liver of zebrafish (*Danio rerio*) across multiple generations. Comp Biochem Physiol C Toxicol Pharmacol. 2021;240:108918.
40. Borowiec BG, Scott GR. Hypoxia acclimation alters reactive oxygen species homeostasis and oxidative status in estuarine killifish (*Fundulus heteroclitus*). J Exp Biol. 2020;223:jeb222877.
41. Li ZX, Wang LX, Zhang Y, Chen W, Zeng YQ. circGLI3 inhibits oxidative stress by regulating the miR-339-5p/VEGFA Axis in IPEC-J2 cells. Biomed Res Int. 2021;2021:1086206.
42. Zhou B, Wu LL, Zheng F, Wu N, Chen AD, Zhou H, et al. Mir-31-5p promotes oxidative stress and vascular smooth muscle cell migration in spontaneously hypertensive rats via inhibiting *FNDC5* expression. Biomedicines. 2021;9:1009.
43. Shi CC, Pan LY, Zhao YQ, Li Q, Li JG. MicroRNA-323-3p inhibits oxidative stress and apoptosis after myocardial infarction by targeting TGF-β2/JNK pathway. Eur Rev Med Pharmacol Sci. 2020;24:6961–70.
44. Hoffmann MS, Singh P, Wolk R, Narkiewicz K, Somers VK. Obstructive sleep apnea and intermittent hypoxia increase expression of dual specificity phosphatase 1. Atherosclerosis. 2013;231:378–83.
45. Liu X, Cai X, Hu B, Mei Z, Zhang D, Ouyang G, et al. Forkhead transcription factor 3a (*FOXO3a*) modulates hypoxia signaling via up-regulation of the Von hippel-lindau gene (*VHL*). J Biol Chem. 2016;291:25692–705.
46. Ding F, Gao F, Zhang S, Lv X, Chen Y, Liu Q. A review of the mechanism of DDIT4 serve as a mitochondrial related protein in tumor regulation. Sci Prog. 2021;104:36850421997273.
47. Yan M, Yang S, Meng F, Zhao Z, Tian Z, Yang P. MicroRNA 199a-5p induces apoptosis by targeting JunB. Sci Rep. 2018;8:6699.
48. Feng J, Zhang Y, She X, Sun Y, Fan L, Ren X, et al. Hypermethylated gene *ANKDD1A* is a candidate tumor suppressor that interacts with FIH1 and decreases HIF1α stability to inhibit cell autophagy in the glioblastoma multiforme hypoxia microenvironment. Oncogene. 2019;38:103–19.
49. Schmidt D, Textor B, Pein OT, Licht AH, Andrecht S, Sator-Schmitt M, et al. Critical role for NF-kappaB-induced JunB in VEGF regulation and tumor angiogenesis. EMBO J. 2007;26:710–9.
50. Ton C, Stamatiou D, Liew CC. Gene expression profile of zebrafish exposed to hypoxia during development. Physiol Genomics. 2003;13:97–106.
51. Hall JR, Short CE, Petersen LH, Stacey J, Gamperl AK, Driedzic WR. Expression levels of genes associated with oxygen utilization, glucose transport and glucose phosphorylation in hypoxia exposed Atlantic Cod (*Gadus morhua*). Comp Biochem Physiol Part D Genomics Proteom. 2009;4:128–38.
52. Cardona E, Milhade L, Pourtau A, Panserat S, Terrier F, Lanuque A, et al. Tissue origin of circulating microRNAs and their response to nutritional and environmental stress in rainbow trout (*Oncorhynchus mykiss*). Sci Total Environ. 2022;853:158584.
53. Ma JL, Qiang J, Tao YF, Bao JW, Zhu HJ, Li LG, et al. Multi-omics analysis reveals the glycolipid metabolism response mechanism in the liver of genetically improved farmed Tilapia (GIFT, *Oreochromis niloticus*) under hypoxia stress. BMC Genomics. 2021;22:105.
54. Zare-Chahoki A, Ahmadi-Zeidabadi M, Azadarmaki S, Ghorbani S, Noorbakhsh F. Inflammation in an animal model of multiple sclerosis leads to microRNA-25-3p dysregulation associated with inhibition of *Pten* and *Klf4*. Iran J Allergy Asthma Immunol. 2021;20:314–25.
55. Liu X, Zhou F, Yang Y, Wang W, Niu L, Zuo D, et al. MiR-409-3p and MiR-1896 co-operatively participate in IL-17-induced inflammatory cytokine production in astrocytes and pathogenesis of EAE mice via targeting SOCS3/STAT3 signaling. Glia. 2019;67:101–12.
56. Fu B, Xie J, Kaneko G, Wang G, Yang H, Tian J, et al. MicroRNA-dependent regulation of targeted mRNAs for improved muscle texture in crisp grass carp fed with broad bean. Food Res Int. 2022;155:111071.
57. Samanta M, Satapathy S, Paichha M, Choudhary P. *Labeo rohita* Mx1 exhibits the critical structural motifs of the family of large GTPases of mammals and is activated by rhabdovirus vaccination and bacterial RNA stimulations. Anim Biotechnol. 2022;33:22–42.
58. Wu S, Huang J, Li Y, Lei M, Zhao L, Liu Z. Integrated analysis of immune parameters, miRNA-mRNA interaction, and immune genes expression in the liver of rainbow trout following infectious hematopoietic necrosis virus infection. Front Immunol. 2022;13:970321.
59. Dong M, Zhu L, Shao B, Zhu S, Wang J, Xie H, et al. The effects of endosulfan on cytochrome P450 enzymes and glutathione S-transferases in zebrafish (*Danio rerio*) livers. Ecotoxicol Environ Saf. 2013;92:1–9.
60. Reynaud S, Raveton M, Ravanel P. Interactions between immune and biotransformation systems in fish: a review. Aquat Toxicol. 2008;87:139–45.
61. Wu S, Huang J, Li Y, Liu Z, Zhao L. Integrated analysis of lncRNA and circRNA mediated ceRNA regulatory networks in skin reveals innate immunity differences between wild-type and yellow mutant rainbow trout (*Oncorhynchus mykiss*). Front Immunol. 2022;13:802731.
62. Ernst J, Bar-Joseph Z. STEM: a tool for the analysis of short time series gene expression data. BMC Bioinformatics. 2006;7:191.
63. Ma F, Liu Z, Huang J, Kang Y, Wang J. Evaluation of reference genes for quantitative real-time PCR analysis of messenger RNAs and microRNAs in rainbow trout *Oncorhynchus mykiss* under heat stress. J Fish Biol. 2019;95:540–54.
64. Wu S, Huang J, Li Y, Liu Z, Zhao L. MiR-382 functions on the regulation of melanogenesis via targeting *dct* in rainbow trout (*Oncorhynchus mykiss*). Mar Biotechnol. 2022;24:776–87.

Publisher's note